Inorg. Chem. **2003**, *42*, 1769–1778

Synthesis and Molecular Structure of the Dihydrobis(thioxotriazolinyl)borato Complexes of Zinc(II), Bismuth(III), and Nickel(II). M···H–B Interaction Studied by Ab Initio Calculations

Roberto Cammi, Maurizio Lanfranchi, Luciano Marchiò,* Clara Mora, Cristiano Paiola, and Maria Angela Pellinghelli

Dipartimento di Chimica Generale ed Inorganica, Chimica Analitica, Chimica Fisica, Università degli Studi di Parma, Parco Area delle Scienze 17/A, 43100 Parma, Italy

Received July 11, 2002

Reacting the heterocycle 5-thioxo-1,4-dihydro-4-ethyl-3-methyl-1,2,4-triazole (thioxotriazoline) with sodium tetrahydroborate in the molar ratio of ~2:1 at 130 °C provides the new ligand dihydrobis(thioxotriazolinyl)borato, $[Bt^{Et,Me}]^-$, as its sodium salt. The neutral complexes of this anionic ligand with zinc(II), bismuth(III), and nickel(II) have been synthesized and characterized by X-ray crystallography. In every complex, the ligand is coordinated to the metal in the S_2 mode, generating eight-membered chelate rings. The bismuth and nickel complexes exhibit two M···H–B interactions responsible for the dodecahedral and octahedral geometries, respectively. For the zinc complex, the trigonal-bipyramidal coordination is achieved with an apical Zn···H–B interaction. The crystal structures for the three complexes are described, and ab initio calculations on Bi(III), Ni(II), and Zn(II) compounds have been performed in order to assess the nature of the M···H–B interaction and its role for the definition of the molecular geometries.

Introduction

The fairly simple procedure employed for the synthesis of the Tp,[1] Tm,[2] and Tt[3] tripodal ligands [Tp = hydrotris(pyrazolyl)borato; Tm = hydrotris(thioxoimidazolyl)borato; Tt = hydrotris(thioxotriazolinyl)borato] can also be adapted to the synthesis of the bis-substitution products in which two penta-atomic rings take the place of two hydrido groups in the tetrahydroborate anion. The only factor that needs to be considered is the molar ratio between the reagents, which has to be 2:1 for an L bearing the N−H group and BH_4^- (L = pyrazole, thioxoimidazole, thioxotriazole). The reaction and purification protocols are then the same as those corresponding to the superior trisubstituted homologous Tp, Tm, and Tt.

The dihydrobis(pyrazolyl)borates, Bp,[1] and dihydrobis(thioxoimidazolyl)borato ligand, Bm,[4] formally act as a bidentate through the pyrazolyl nitrogen atoms (N_2 mode) or by means of the thione groups (S_2 mode), respectively. Moreover, the Bp ligands are known to display agonistic M···H−B interactions toward a wide range of transition-metal ions,[5] and a similar interaction was also found for the *softer* Bm ligands toward the zinc and thallium cations[4,6] (Scheme 1). The evidence of this interaction, involving one of the two hydrido groups, poses interesting chemical and spectroscopic problems.[7] This interaction is related to the electronic configuration of the metals, to the influence of the ligand substituents, to the flexibility and conformation of the chelating rings (six-, seven-, and eight-membered

* Author to whom correspondence should be addressed. E-mail: marchio@unipr.it.

(1) Trofimenko, S. *Chem. Rev.* **1993**, *93*, 943−980.
(2) (a) Reglinski, J.; Garner, M.; Cassidy, I.; Slavin, P. A.; Spicer, M. D.; Armstrong, D. *J. Chem. Soc., Dalton Trans.* **1999**, 2119−2126. (b) Garner, M.; Reglinski, J.; Cassidy, I.; Spicer, M. D.; Kennedy, A. *Chem. Commun*. **1996**, 1975−1976.
(3) Bailey, P. J.; Lanfranchi, M.; Marchiò, L.; Parsons, S. *Inorg. Chem.* **2001**, *19*, 5030−5035.
(4) Kimblin, C.; Bridgewater, B. M.; Hascall, T.; Parkin, G.; *J. Chem. Soc., Dalton Trans.* **2000**, 891−897.
(5) (a) Leonor, M.; Campello, M. P.; Domingos, A.; Santos, I.; Andersen, R. *J. Chem. Soc., Dalton Trans.* **1999**, 2015−2020. (b) Chowdhury, S. K.; Samanta, U.; Puranik, V. G.; Sarkar, A. *Organometallics* **1997**, *16*, 2618−2622. (c) Rasika Dias, H. V.; Gorden, J. D. *Inorg. Chem.* **1996**, *35*, 318−324. (d) Rasika Dias, H. V.; Lu, H.; Gorden, J. D.; Jin, W. *Inorg. Chem.* **1996**, *35*, 2149−2151. (e) Albers, M. O.; Crosby, F. A.; Liles, D. C.; Robinson, D. J.; Shaver, A.; Singleton, E. *Organometallics* **1987**, *6*, 2014−2017. (f) Rodriguez, V.; Full, J.; Donnadieu, B.; Sabo-Etienne, S.; Chaudret, B. *New J. Chem.* **1997**, *21*, 847−849. (g) Reger, D. L.; Mathab, R. J.; Baxter, C.; Lebioda, L. *Inorg. Chem.* **1986**, *25*, 2046−2048.
(6) Kimblin, C.; Hascall, T.; Parkin, G. *Inorg. Chem.* **1997**, *36*, 5680−5681.
(7) (a) Reger, D. L.; Lindeman, J. A.; Lebioda, L. *Inorg. Chem.* **1988**, *27*, 1890−1896. (b) Reger, D. L.; Chou, T.; Studer, S. L.; Steven, S. L.; Knox, S. J.; Martinez, M. L. *Inorg. Chem.* **1991**, *30*, 2397−2402.

10.1021/ic025870r CCC: $25.00
Published on Web 02/13/2003

Scheme 1

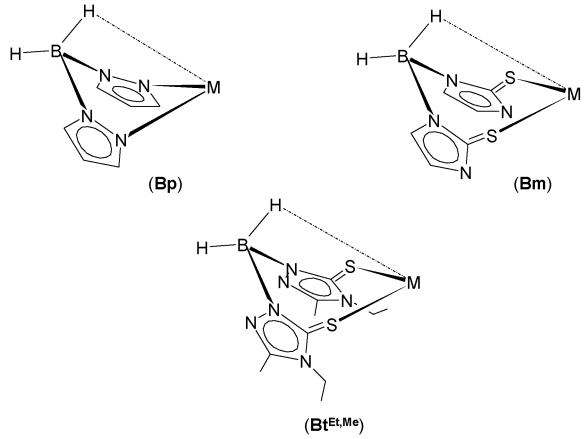

rings), and to the nature of the ligating atoms (N or S). It is, therefore, difficult to rationalize and predict when this interaction can occur and to define "a priori" the coordination geometry.

If this intramolecular M···H−B interaction is considered, the Bp and Bm ligands can be regarded as "hidden" tripods, coordinating in the N,N,H and S,S,H modes, respectively. In fact, it has been recently reported that the nickel complex $Ni(Bm^{Me})_2$ exhibits this peculiar interaction in which the octahedral coordination is achieved through two Ni···H−B interactions in the cis position and each ligand is S,S,H coordinated.[8]

Herein we report the coordination properties of the new, potentially ambidentate N_2/S_2, dihydrobis(thioxotriazolinyl)-borato ligand $Bt^{Et,Me}$ [the superscript indicates the substituents on the thioxotriazolinyl rings; the first fragment is relative to the substituent on the N(3) nitrogen atom, whereas the second is for the substituent on the C(2) carbon atom] with the zinc(II), bismuth(III), and nickel(II) cations (Scheme 1).

As reported in many publications, ab initio calculations are fundamental for the study of various kinds of intramolecular interactions.[9] We have adopted the same techniques in order to establish the role and nature of this interaction in the definition of the complex geometry coordination.

The large dimensions of our molecules suggest the use of ab initio mixed techniques[10−16] that allow for a reduction of the computational effort without a significant loss in accuracy. Two-layer ONIOM[15,16] calculations have been performed on the Ni(II) and Bi(III) complexes to obtain the equilibrium geometries for comparison with the experimental X-ray structures. The same calculations were performed on the Zn(II) complex, but the resulting equilibrium geometry did not correspond to the experimental one. A further B3LYP/LANL2DZ single-point calculation on the equilibrium geometries for the Bi(III) and Ni(II) complexes and on the experimental geometry for the Zn(II) complex has been used to supply an accurate wave function to the successive "atoms in molecules" (AIM)[17,18] electron-density-distribution analysis. The AIM topological analysis of the electron-density distribution confirms the fundamental role of the M···H−B interaction in the coordination geometry and allows us to name it as an "inverse hydrogen bond"[19] and not as an agonistic interaction.

Experimental Section

General Procedures. All solvents and reagents are commercially available and were used as received. The ^1H spectra were recorded on a Bruker 300 spectrometer operating at room temperature. Chemical shifts are reported in ppm, referenced to residual solvent protons. Mass spectra were run on a Quattro LC (Micromass, Manchester, U.K.) triple quadrupole mass spectrometer in positive- and negative-ion mode with a pneumatically assisted electrospray ionization (ESI) interface and on a Finnigan 1020 mass spectrometer in positive-ion mode with a MATSS 710 quadrupole. Infrared spectra were recorded as KBr pellets from 4000 to 400 cm^{-1} on a Perkin-Elmer FT-IR Nexus spectrometer.

Preparation of 5-Thioxo-1,4-dihydro-4-ethyl-3-methyl-1,2,4-triazole. In a 100-mL round-bottomed flask, 4-ethyl-3-thiosemicarbazide (10.9 g, 91.5 mmol) was heated to reflux for 3 days in glacial acetic acid (45 mL). The solution was then concentrated to half of the original volume by vacuum distillation. Upon cooling, a white solid precipitated, which was filtered and washed with cold water (20 mL). The product was then dissolved in hot water (ca. 100 mL) and extracted into chloroform (8 × 50 mL) in a separating funnel. The $CHCl_3$ solution was concentrated under a reduced pressure, and a yellow product was collected (4.1 g, 28 mmol, 31%). Mp: 116−117 °C. IR (KBr disk, cm^{-1}): 3111s, 3060m, 2954s, 1575s, 1499s, 1364s, 1087s, 797m, 694m. ^1H NMR ($CDCl_3$): δ 1.31 (t, 3H, CH_3), 2.30 (s, 3H, CH_3), 4.02 (q, 2H, CH_2), 9.45 (s, N−H). MS (*m*/*z*, I%): 143, 100 [M^+]. Anal. Calcd for $C_5H_9N_3S$: C, 41.94; H, 6.34; N, 29.37. Found: C, 41.34; H, 6.40; N, 28.66.

Preparation of Sodium Dihydrobis(thioxotriazolinyl)borate Trihydrate, $NaBt^{Et,Me}\cdot 3H_2O$ (1). 5-Thioxo-1,4-dihydro-4-ethyl-3-methyl-1,2,4-triazole (3.49 g, 24.4 mmol) and sodium tetrahydroborate (0.430 g, 11.4 mmol) were mixed together in a 100-mL round-bottomed flask fitted to a volumetric device for measuring hydrogen evolution. Upon stirring, the temperature was raised gently to 130 °C, whereupon the mixture melted and evolution of the hydrogen gas began. The mixture was stirred at this temperature for 1.5 h when 2 equiv of dihydrogen had evolved (ca. 500 mL). The reaction mixture was allowed to cool to room temperature. The resulting yellow, glassy solid was inserted in the thimble of a Soxhlet apparatus and washed with chloroform for 4 h. From the thimble, a powdery white product was collected. The product is hygroscopic, and contact with moist air provided the hydrated form **1** (2.11 g, 5.64 mmol, 49%). IR (KBr disk, cm^{-1}): 3372s, 2987s, 2948s, 2417m, 2395s, 2353m, 1575s, 1469s, 1421s, 1130s, 1043s,

(8) Alvarez, H. M.; Krawiec, M.; Donovan-Merkert, B. T.; Fouzi, M.; Rabinovich, D. *Inorg. Chem.* **2001**, *40*, 5736−5737.
(9) Shishkin, O. V.; Gorb, L.; Leszczynski, J. *Int. J. Mol. Sci.* **2000**, *1*, 17−27.
(10) Alkorta, I.; Elguero, J. *J. Am. Chem. Soc.* **2002**, *124*, 1488−1493.
(11) Cuevas, G. *J. Am. Chem. Soc.* **2000**, *122*, 692−698.
(12) Philipp, D. M.; Friesner, R. A. *J. Comput. Chem.* **1999**, *20*, 1468−1494.
(13) Gogonea, V.; Westerhoff, L. M.; Kenneth, M. M., Jr. *J. Chem. Phys.* **2000**, *14*, 5604−5613.
(14) Bakowies, D.; Thiel, W. *J. Phys. Chem.* **1996**, *100*, 10580−10594.
(15) Svensson, M.; Humbel, S.; Froese, R. D. J.; Matsubara, T.; Sieber, S.; Morokuma, K. *J. Phys. Chem.* **1996**, *100*, 19357−19363.
(16) Dapprich, S.; Komaromi, I.; Byun, K. S.; Morokuma, K.; Frisch, M. J. *J. Mol. Struct.* **1999**, *461*−*462*, 1−21.
(17) Bader, R. F. W. *Atoms in Molecules*; Oxford University Press: Oxford, 1990.
(18) Bader, R. W. F. *Chem. Rev.* **1991**, *91*, 893.
(19) Desiraju, G. R.; Steiner, T. *The Weak Hydrogen Bond in Structural Chemistry and Biology*; IUCr Monographs on Crystallography: Oxford, 1999.

Table 1. Summary of Crystallographic Data for Compounds **2a**, **3**, and **4a**

	2a	**3**	**4a**
empirical formula	$C_{22}H_{39}B_2N_{13}S_4Zn$	$C_{30}H_{54}B_3BiN_{18}S_6$	$C_{22}H_{41}B_2N_{13}NiOS_4$
fw	700.89	1100.68	712.25
color, habit	colorless, block	orange, block	green, block
cryst size, mm	0.38 × 0.30 × 0.25	0.35 × 0.22 × 0.15	0.40 × 0.35 × 0.15
cryst syst	monoclinic	triclinic	triclinic
space group	$P2_1/n$	$P\bar{1}$	$P\bar{1}$
a, Å	16.697(1)	12.118(1)	13.631(1)
b, Å	9.091(1)	12.132(1)	15.307(1)
c, Å	22.663(2)	17.808(2)	17.560(1)
α, deg	90	73.253(2)	96.038(2)
β, deg	92.598(2)	85.476(2)	96.168(2)
γ, deg	90	71.724(2)	103.786(2)
V, Å^3	3436.6(5)	2380.4(4)	3505.1(4)
Z	4	2	4
T, K	293(2)	293(2)	293(2)
λ(Mo Kα), Å	0.710 73	0.710 73	0.710 73
ρ(calc), mg/m^3	1.355	1.536	1.350
μ, mm^{-1}	0.993	4.011	0.830
θ range, deg	1.55−24.00	1.19−26.04	1.18−26.12
no. reflns/obsd $F > 4\sigma(F)$	16 039/2577	13 426/6302	22 158/6608
R1[a]	0.0409	0.0398	0.0506
wR2[b]	0.0581	0.0593	0.1096

[a] $R1 = \sum||F_o| - |F_c||/\sum|F_o|$. [b] $wR2 = \{\sum[w(F_o^2 - F_c^2)^2]/\sum[w(F_o^2)^2]\}^{1/2}$; $w = 1/[\sigma^2(F_o^2) + (aP)^2 + bP]$, where $P = [\max(F_o^2,0) + 2F_c^2]/3$.

870m, 772m, 493m. ^{1}H NMR (DMSO-d_6): δ 1.14 (t, 3H, CH_3), 2.20 (s, 3H, CH_3), 3.91 (q, 2H, CH_2). ESI-MS (*m*/*z*, I%): 297, 100 [$Bt^{Et,Me}$]$^-$. Anal. Calcd for $C_{10}H_{18}BN_6NaS_2\cdot 3(H_2O)$: C, 32.09; H, 6.46; N, 22.45. Found: C, 32.65; H, 5.91; N, 22.55.

Preparation of {Bis(dihydrobis(thioxotriazolinyl)borato)}-zinc(II), Zn($Bt^{Et,Me}$)$_2$ (2). $ZnSO_4\cdot 7H_2O$ (0.100 g, 0.348 mmol) was dissolved in methanol (10 mL) and was added to a methanolic (20 mL) solution of **1** (0.259 g, 0.692 mmol). The white suspension formed was stirred at room temperature for 3 h. The suspension was filtered, and the white powder of $Zn(Bt^{Et,Me})_2$ was collected (0.110 g, 0.167 mmol, 48%). Recrystallization of the white powder from an acetonitrile solution gave white, colorless crystals structurally characterized by X-ray crystallography as $[Zn(Bt^{Et,Me})_2]\cdot CH_3CN$ (**2a**). IR (KBr disk, cm^{-1}): 2987m, 2948m, 2446s, 2362m, 1563s, 1576s, 1429s, 1375s, 1270s, 1137s, 875m. ^{1}H NMR ($CDCl_3$): δ 1.17 (t, 3H, CH_3), 2.35 (s, 3H, CH_3), 3.93 (q, 2H, CH_2). ESI-MS (*m*/*z*, I%): 661, 35 [M + 1]$^+$; 683, 100 [M + 23]$^+$. Anal. Calcd for $C_{20}H_{36}B_2N_{12}S_4Zn\cdot(CH_3CN)$: C, 37.69; H, 5.61; N, 25.98. Found: C, 37.55; H, 5.45; N, 25.63.

Preparation of {Tris(dihydrobis(thioxotriazolinyl)borato)}-bismuth(III), Bi($Bt^{Et,Me}$)$_3$ (3). $Bi(NO_3)_3\cdot 5H_2O$ (0.220 g, 0.454 mmol) was dissolved in methanol (20 mL) and was added to a methanolic (20 mL) solution of **1** (0.450 g, 1.26 mmol). The resulting orange mixture was stirred at room temperature for 5 h. The solvent was then removed under vacuum, the red powder was dissolved in acetonitrile (30 mL), and the sodium nitrate was eliminated by filtration. The solvent was removed under vacuum from the orange solution, and $Bi(Bt^{Et,Me})_3$ was collected (0.310 g, 0.282 mmol, 62%). IR (KBr disk, cm^{-1}): 2973m, 2933m, 2429s, 2347w, 1564s, 1429s, 1375s, 1270s, 1137s, 875m. ^{1}H NMR ($CDCl_3$): δ 1.20 (t, 3H, CH_3), 2.35 (s, 3H, CH_3), 3.92 (q, 2H, CH_2). ESI-MS (*m*/*z*, I%): 803, 100; 1102, 27 [M$^+$]; 1124, 95 [M + 23]$^+$. Anal. Calcd for $C_{30}H_{54}B_3BiN_{18}S_6$: C, 32.73; H, 4.94; N, 22.90. Found: C, 32.25; H, 4.64; N, 22.38. Recrystallization of the reddish powder from an acetonitrile solution gave orange crystals structurally characterized by X-ray crystallography as $Bi(Bt^{Et,Me})_3$ (**3**).

Preparation of {Bis(dihydrobis(thioxotriazolinyl)borato)}-nickel(II), Ni($Bt^{Et,Me}$)$_2$ (4). $NiCl_2\cdot 6H_2O$ (0.080 g, 0.337 mmol) was dissolved in methanol (10 mL) and was added to a methanolic (20 mL) solution of **1** (0.240 g, 0.641 mmol). The green suspension was stirred at room temperature for 1 h. The solvent was removed under vacuum, and the green powder was dissolved in acetonitrile (30 mL) and the sodium chloride removed by filtration. The solvent was removed from the resulting green solution, and **4** was collected (0.210 g, 0.322 mmol, 96%). IR (KBr disk, cm^{-1}): 2976m, 2933m, 2464m, 2364m, 2244m, 2197m, 1569s, 1468s, 1381s, 1274s, 1274s, 848m. IR (CH_2Cl_2 solution, cm^{-1}) 2463m, 2364m, 2244m, 2198m. ^{1}H NMR (CD_3CN): δ 1.1 (br), 2.4 (br), 6.1 (br). Anal. Calcd for $C_{20}H_{36}B_2N_{12}NiS_4$: C, 36.77; H, 5.56; N, 25.73. Found: C, 37.15; H, 5.74; N, 25.16. Recrystallization of the green powder from an acetonitrile/water solution gave green crystals structurally characterized by X-ray crystallography as $[Ni(Bt^{Et,Me})_2]\cdot CH_3CN\cdot H_2O$ (**4a**).

X-ray Crystallography. Crystals of dimensions 0.38 × 0.30 × 0.25 mm (**2a**, colorless), 0.35 × 0.22 × 0.15 mm (**3**, orange), and 0.40 × 0.35 × 0.15 mm (**4a**, green) were mounted on a glass fiber on a Bruker AXS Smart 1000 area-detector diffractometer. Graphite-monochromated Mo Kα (λ = 0.710 73 Å) radiation was used. The intensity data were collected using the $\omega-2\theta$ scan technique. No crystal decay was observed; an absorption correction was applied using the program SADABS,[20] which resulted in transmission factors ranging from 0.82 to 1.00, 0.78 to 1.00, and 0.69 to 1.00, respectively. The structures were solved by direct methods (SIR97)[21] and refined with full-matrix least squares (SHELXL-97),[22] using the Wingx software package.[23] Nonhydrogen atoms were refined anisotropically, and the hydrogen atoms were placed at their calculated positions, which were found and refined for all compounds except for BH_2. In **4a**, three independent acetonitrile (two of which were found to be disordered with a Site Occupancy Factor of 0.5) and three water (two of which were found to be disordered with a Site Occupancy Factor of 0.5) solvation molecules were found. The maximum and minimum peaks on the final-difference Fourier maps corresponded to +0.370 and −0.276 e Å^{-3} for **2a**, +0.855 and −1.000 e Å^{-3} for **3**, and +0.543 and −0.340 e Å^{-3} for **4a**. Crystallographic data are summarized in Table 1, and selected bond lengths and angles are listed in Table 2. The programs

(20) *Area-Detector Absorption Correction*; Siemens Industrial Automation, Inc.: Madison, WI, 1996.
(21) Altomare, A.; Burla, M. C.; Camalli, M.; Cascarano, G. L.; Giacovazzo, C.; Guagliardi, A.; Moliterni, A. G. G.; Polidori, G.; Spagna, R. *J. Appl. Crystallogr.* **1999**, *32*, 115−119.
(22) Sheldrick, G. M. *SHELX-97: Programs for Crystal Structure Analysis*, Release 97−2; University of Göttingen: Göttingen, Germany, 1997.
(23) Farrugia, L. J. *J. Appl. Crystallogr.* **1999**, *32*, 837−838.

Table 2. Selected Experimental Bond Lengths (Å) and Angles (deg) with the Estimated Standard Deviation (esd) in Parentheses for **2a**

	X-ray		X-ray
Zn−S(1)	2.402(1)	B(1)−H(1)	1.15(3)
Zn−S(2)	2.328(1)	B(1)−H(2)	1.14(3)
Zn−S(3)	2.300(1)	B(2)−H(3)	1.12(3)
Zn−S(4)	2.351(1)	B(2)−H(4)	1.12(3)
C(11)−S(1)	1.705(4)		
C(12)−S(2)	1.710(4)		
C(13)−S(3)	1.710(4)		
C(14)−S(4)	1.703(4)		

	X-ray		X-ray
S(1)−Zn−S(2)	107.74(5)	S(2)−Zn−S(4)	105.54(4)
S(1)−Zn−S(3)	106.00(5)	S(3)−Zn−S(4)	122.67(5)
S(1)−Zn−S(4)	92.18(5)	H(1)−B(1)−H(2)	112(2)
S(2)−Zn−S(3)	118.65(5)	H(3)−B(2)−H(4)	112(2)

Parst[24] and ORTEP[25] were also used. Full tables of bond lengths and angles, atomic positional parameters, and anisotropic displacement parameters are given in Supporting Information, and details of the crystal structure investigations (excluding structure factors) are deposited in the Cambridge Crystallographic Data Centre as supplementary publication no. CCDC−203228-203230.

Molecular Orbital Calculations. Transition-metal complexes require accurate techniques to reliably describe their properties. Density-functional methods with hybrid functionals such as B3LYP, coupled with the double-ζ basis set, are the most commonly used for their reasonable compromise between accuracy and computational demand.

To reduce the computational effort without a significant loss in accuracy, we have also decided to use the ONIOM method of Morokuma and co-workers.[15,16]

In the determination of the equilibrium geometries for Ni(II) and Bi(III) complexes for comparison with the X-ray crystal structures, we have used the two-layer ONIOM technique also known as IMOMO.[26] The gradient-corrected hybrid density-functional B3LYP[27,28] method and double-ζ basis set LANL2DZ with Hay-and-Wadt effective core potential (ECP)[29,30] have been used for the description of the "model system". Hartree−Fock with a minimum basis set LANL2MB with Hay and Wadt ECP[29,30] has been used for the "real system". In the basis set for the model, we added a polarization p function for both hydrogens bonded to the boron atoms and a polarization d function for all the sulfur atoms to better describe their interactions with the metal center. The details about the ONIOM layers defined for the molecules are reported in Figure 1.

A single-point calculation for all complexes using the same level of theory as the "model system" layer was performed in order to obtain a good-quality wave function to submit to the AIM analysis.[17,18] All the calculations have been performed with Gaussian 01.[31]

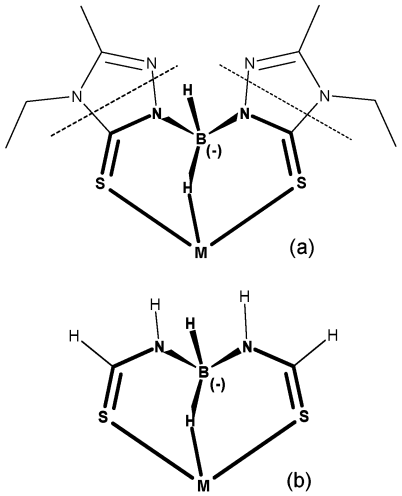

Figure 1. ONIOM partitioning scheme adopted for a (a) "real system" and (b) "model system".

Because of the limitations of the AIM2000 Release 1 package[32,33] used for the AIM analysis that allows a maximum of 100 atoms, we have used the structure named $Bi(Bt^{Me,Me})_3$ obtained by substituting the ethyl groups with methyl groups in the bismuth complex **3** to calculate the wave function. The absence of significant disagreement between the atomic charges of **3** and $Bi(Bt^{Me,Me})_3$ obtained with the natural bond-orbital (NBO) theory[34,35] has allowed us to confirm the goodness of this modification. The results of this comparison are reported in Table 9.

Results and Discussion

The $Bt^{Et,Me}$ ligand can ideally act as a N_2/S_2 bidentate by virtue of the triazoline nitrogen atoms and of the thione groups, as already shown for its parent superior homologous Tt,[3] and its sodium salt could be formulated as **1** by means of microanalysis and spectroscopy. The product is air-stable, soluble in water, and moderately soluble in methanol and dimethyl sulfoxide, but it is not soluble in chloroform.

To investigate the coordination properties of the $Bt^{Et,Me}$, reactions with $ZnSO_4 \cdot 7H_2O$ (molar ratio 2:1 L/M), $Bi(NO_3)_3 \cdot 5H_2O$ (molar ratio 3:1 L/M), and $NiCl_2 \cdot 6H_2O$ (molar ratio 2:1 L:M) have been performed in methanol. The metal ions have been chosen to dispose a wide range of coordination numbers and polyhedra. The Zn(II) cation can give equally stable tetrahedral and octahedral complexes, whereas Ni(II) is more likely to adopt square-planar and octahedral geometries.[36] As for the Bi(III) ion, it can present various coordination numbers (3−10), and the potentially active lone

(24) (a) Nardelli, M. *Comput. Chem.* **1983**, *7*, 95. (b) Nardelli, M. *J. Appl. Crystallogr.* **1995**, *28*, 659.
(25) Farrugia, L. J. *J. Appl. Crystallogr.* **1997**, *30*, 565.
(26) Humbel, S.; Sieber, S.; Morokuma, K. *J. Chem. Phys.* **1996**, *105*, 1959−1967.
(27) Becke, A. D. *Phys. Rev. A: At., Mol., Opt. Phys.* **1988**, *38*, 3098.
(28) Becke, A. D. *J. Chem. Phys.* **1993**, *98*, 5648.
(29) Hay, P. J.; Wadt, W. R. *J. Chem. Phys.* **1985**, *82*, 299.
(30) Wadt, W. R.; Hay, P. J. *J. Chem. Phys.* **1985**, *82*, 284.
(31) Frisch, M. J.; Trucks, G. W.; Schlegel, H. B.; Scuseria, G. E.; Robb, M. A.; Cheeseman, J. R.; Zakrzewski, V. G.; Montgomery, J. A., Jr.; Kudin, K. N.; Burant, J. C.; Millam, J. M.; Stratmann, R. E.; Tomasi, J.; Barone, V.; Mennucci, B.; Cossi, M.; Scalmani, G.; Rega, N.; Iyengar, S.; Petersson, G. A.; Ehara, M.; Toyota, K.; Nakatsuji, H.; Adamo, C.; Jaramillo, J.; Cammi, R.; Pomelli, C.; Ochterski, J.; Ayala, P. Y.; Morokuma, K.; Salvador, P.; Dannenberg, J. J.; Dapprich, S.; Daniels, A. D.; Strain, M. C.; Farkas, O.; Malick, D. K.; Rabuck, A. D.; Raghavachari, K.; Foresman, J. B.; Ortiz, J. V.; Cui, Q.; Baboul, A. G.; Clifford, S.; Cioslowski, J.; Stefanov, B. B.; Liu, G.; Liashenko, A.; Piskorz, P.; Komaromi, I.; Gomperts, R.; Martin, R. L.; Fox, D. J.; Keith, T.; Al-Laham, M. A.; Peng, C. A.; Nanayakkara, A.; Challacombe, M.; Gill, P. M. W.; Johnson, B.; Chen, W.; Wong, M. W.; Andres, J. L.; Gonzalez, C.; Head-Gordon, M.; Replogle, E. S.; Pople, J. A. *Gaussian 01, Development Version*, Revision B.01; Gaussian, Inc.: Pittsburgh, PA, 2001.
(32) http://gauss.fh-bielefeld.de/aim2000.
(33) Boegler-König, F.; Schönbohm, J.; Bayles, D. *J. Comput. Chem.* **2001**, *22*, 545−559.
(34) Reed, A. E.; Weinhold, F. *J. Chem. Phys.* **1983**, *78*, 4066−4073.
(35) Reed, A. E.; Weinstock, R. B.; Weinhold, F. *J. Chem. Phys.* **1985**, *83*, 735−746.

pair ($6s^2$) can have a relevant stereochemical role.[37] All the complexes are moderately soluble in methanol, dimethyl sulfoxide, acetonitrile, and chloroform, but they are insoluble in water. The solubility of the bismuth and nickel complexes in acetonitrile allowed the purification of the reaction products from the inorganic salts upon extraction in this solvent. Satisfactory elemental analyses have been performed for all complexes, and they could be formulated as **2**, **3**, and **4**, respectively. The coordination modes (N_2 or S_2) adopted by the ligand greatly depend on the nature of the metal, and for the bismuth complex, it was not hazardous to venture into the S_2 mode. The same could not be said for the nickel and zinc complexes because both modes could be accessible. Spectroscopic evidence was not sufficient to provide enough insight for the definition of the coordination mode which was determined by means of X-ray structural analysis for the three complexes.

Molecular Structures. The molecular structures of the three complexes are reported in Figures 2−4, and selected bond distances and angles are listed in Table 2. For all the complexes, every $Bt^{Et,Me}$ binds the metal in the S_2 mode, generating eight-membered chelate rings. Thus, the preference of the considered metals for the thione functionality over the triazolinic nitrogen atoms is indicated, even though in this latter case six-membered chelate rings would be formed.

The conformations of the eight-membered chelate rings can be described using the same conformational descriptors for the six-membered rings because the fragment S−C−N−B is planar. In fact, the eight-membered rings can be thought of as six-membered, whereby two of their vertexes are occupied by the triazoline centroids (Scheme 2). For the complexes considered, the possible conformations are twist, boat, and chair. For this last conformation, any M···H−B interaction is prevented because the BH_2 fragment would point away from the metal center.

The zinc complex **2** crystallizes in the monoclinic space group $P2_1/n$, and the metal is bound by four sulfur atoms from two ligands in a severely distorted tetrahedral geometry. The Zn−S bond lengths vary from 2.300(1) to 2.402(1) Å, and the bond angles range from 92.18(5) to 122.67(5)°. The considerable distortion from the theoretical geometry can be explained by considering a very weak interaction between the metal atom and the H4 atom from a borohydride moiety that renders the overall geometry nearly trigonal bipyramidal [the apexes are represented by the S(1) and H(4) atoms; Figure 2], even though this separation of 2.57(3) Å is longer if compared to the range of the Zn···H−B interactions found in the Cambridge Structural Database (1.73−2.41 Å); moreover, the Zn−S bond distance [2.402(1) Å] is significantly longer for the sulfur atom trans to the H(4) hydride (Table 2) if compared to the other Zn−S bond distances [av 2.326(1) Å], and the S(1)−Zn−H(4) angle [169(7)°] is close to the theoretical value of 180° for a trigonal bypyramid.

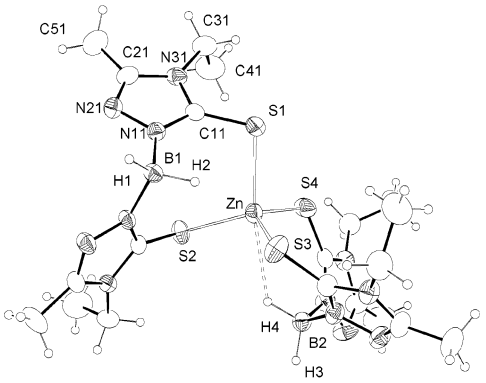

Figure 2. ORTEP drawing of **2** with 30% thermal ellipsoids.

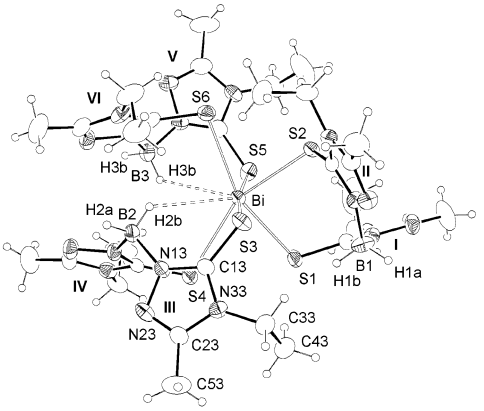

Figure 3. ORTEP drawing of **3** with 30% thermal ellipsoids.

Scheme 2

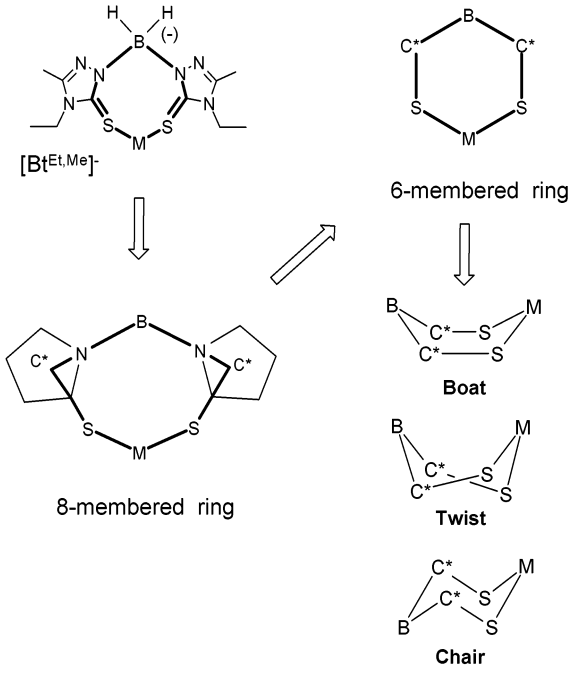

From analysis of the torsion angles (Supporting Information), each chelating ring adopts a twist conformation.

The bismuth complex crystallizes in the triclinic space group $P\bar{1}$, and the structure of **3**, at first glance, appeared as a distorted octahedron bound by three $Bt^{Et,Me}$ ligands through the sulfur atoms (S_2 mode) (Figure 3). Nevertheless, if two long Bi···H−B interactions [Bi−H(2b) = 3.03(4) Å, Bi−

(36) Greenwood, N. N.; Earnshaw, A. *Chemistry of the Elements*, 2nd ed.; Butterworth Heinmann: Woburn, MA, 1998.
(37) Sadler, P. J.; Li, H.; Sun, H. *Coord. Chem. Rev.* **1999**, *185−186*, 689−709.

H(3b) = 2.92(4) Å] are taken into account, the overall geometry can be considered dodecahedral [the vertexes of the two flattened tetrahedron describing the dodecahedron are defined by S(1), S(2), H(2b), and H(3b) and S(3), S(4), S(5), and S(6)]. Even though these interactions seem to be very weak, asymmetrical B−H distances are envisaged for the B(2) and B(3) borohydrido groups, which are involved in the metal interaction longer. In summary, of the three $Bt^{Et,Me}$ ligands, two behave as S,S,H tripods, whereas the third acts only as a S_2 bidentate. In the latter, the B(1)−H distances are, in fact, more equivalent (Table 2). The Bi−S bond lengths range from 2.753(2) to 2.965(2) Å, and the S−Bi−S angles are consistent with the dodecahedral geometry (Table 2).

As already found for the zinc complex, the three chelating rings adopt a twist conformation.

A more evident M···H−B interaction, displayed by $Bt^{Et,Me}$, appears in its complex with the Ni(II) cation.

The strong preference of Ni(II) to adopt the square-planar geometry is evident in its complexes with the Bp ligands,[38] and if monodentate ligands or ancillary groups on the pyrazolyl rings are present, it can also exhibit the octahedral geometry.[39] In the absence of these latter donor groups, an octahedral coordination can be achieved by two trans Ni···H−B interactions, as found for the recently reported compounds $Ni(Bp^{t-Bu})_2$ and $Ni(Bp^{t-Bu,Me})_2$[40] and other transition-metal complexes.[41] The reasonable expected coordination around the metal for **4** would have been square planar N_4/S_4 or octahedral with two trans Ni···H−B interactions, but the square-planar hypothesis was in contrast with the green color of the product in the solid state and in solution and with anomalous ^{1}H NMR chemical shifts and line widths that were indicative of its paramagnetic octahedral nature. The compound **4a** crystallizes in the triclinic space group $P\bar{1}$, and in the cell, two crystallographically independent complexes of **4** with water and acetonitrile molecules of solvation, partially disordered, were found. The X-ray analysis revealed the unusual bisphenoidal disposition of four sulfur atoms and a cis arrangement of two borohydrido groups, as was reported for the complex $Ni(Bm)_2$.[7] The ligand is, in fact, acting as a S,S,H tripod, forming an eight-membered chelate ring and two six-membered chelate rings (Figure 4).

The complexes are chiral, displaying only a pseudo C_2 symmetry, but the space group is centrosymmetric, so both enantiomers are present. The Ni−H distances range from 1.81(3) to 1.89(3) Å and are comparable to those found in other borohydrido nickel derivatives[42] and in the complex $Ni(Bm^{Me})_2$ [1.863(9) Å] but are significantly longer than a terminal Ni(II)−H (hydride) bond (1.37−1.65 Å, Cambridge Structural Database). The S−Ni bond lengths are not equivalent, with those trans to the borohydrido groups being significantly shorter than the axial ones in both complexes; a greater trans influence of the thioxo sulfur atom compared to the borohydrido fragment can thus be inferred.

Even though the two independent molecules display the same coordination environment, they exhibit significant differences in the conformations of the chelating rings, which are predominantly of the *boat* type for molecule I and intermediate between *boat* and *twist* for molecule II.

In Table 3, the geometric parameters describing the agonistic interactions found for the three complexes are reported. The increasing value of the M···H−B angle is in accordance with the increasing strength of the M···H interaction.

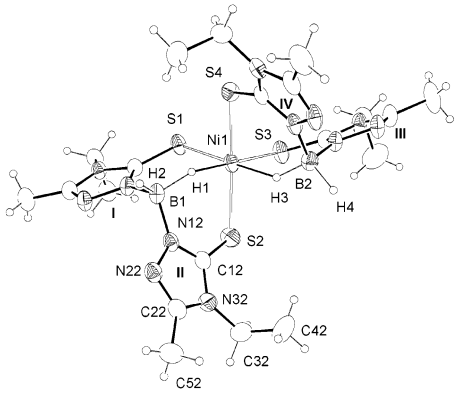

Figure 4. ORTEP drawing of the first independent complex (molecule I) of **4** with 30% thermal ellipsoids.

Table 3. Selected Experimental and Calculated Bond Lengths (Å) and Angles (deg) with the esd in Parentheses for **3**

	X-ray	calcd		X-ray	calcd
Bi−S(1)	2.853(2)	2.955	B(1)−H(1a)	1.14(5)	1.196
Bi−S(2)	2.753(2)	2.918	B(1)−H(1b)	1.10(4)	1.204
Bi−S(3)	2.816(1)	2.911	B(2)−H(2a)	0.91(4)	1.205
Bi−S(4)	2.965(2)	2.925	B(2)−H(2b)	1.09(4)	1.204
Bi−S(5)	2.827(2)	2.943	B(3)−H(3a)	1.01(5)	1.208
Bi−S(6)	2.852(1)	2.982	B(3)−H(3b)	1.16(3)	1.204
C(11)−S(1)	1.722(6)	1.723			
C(12)−S(2)	1.736(5)	1.725			
C(13)−S(3)	1.711(6)	1.724			
C(14)−S(4)	1.697(5)	1.724			
C(15)−S(5)	1.726(6)	1.724			
C(16)−S(6)	1.699(6)	1.724			

	X-ray		X-ray
S(1)−Bi−S(2)	85.19(4)	S(3)−Bi−S(4)	90.85(4)
S(1)−Bi−S(3)	100.09(5)	S(3)−Bi−S(5)	170.46(5)
S(1)−Bi−S(4)	71.47(4)	S(3)−Bi−S(6)	92.24(4)
S(1)−Bi−S(5)	76.55(5)	S(4)−Bi−S(5)	96.42(5)
S(1)−Bi−S(6)	156.20(5)	S(4)−Bi−S(6)	129.04(4)
S(2)−Bi−S(4)	155.61(4)	S(5)−Bi−S(6)	87.97(4)
S(2)−Bi−S(5)	84.58(5)	H(1a)−B(1)−H(1b)	128(4)
S(2)−Bi−S(6)	75.31(4)	H(2a)−B(2)−H(2b)	108(4)
		H(3a)−B(3)−H(3b)	118(3)

(38) (a) Echols, H. M.; Dennis, D. *Acta Crystallogr., Sect. B* **1976**, *32*, 1627. (b) Kokusen, H.; Sohrin, Y.; Matsui, M.; Hata, Y.; Hasegawa, H. *J. Chem. Soc., Dalton Trans.* **1996**, 195−202.

(39) (a) Rheingold, A. L.; Haggerty, B. S.; Liable-Sands, L. M.; Trofimenko, S. *Inorg. Chem.* **1999**, *38*, 6306−6308. (b) Janiak, C.; Sharmann, T. G.; Gunther, W.; Girgsdies, F.; Hemling, H.; Hinrichs, W.; Lenz, D. *Chem.—Eur. J.* **1995**, *1*, 637.

(40) Belderrain, T. R.; Paneque, M.; Carmona, E.; Gutierrez-Puebla, E.; Monge, M. A.; Ruiz-Valero, C. *Inorg. Chem.* **2002**, *41*, 425−428.

(41) Ghosh, P.; Bonanno, J. B.; Parkin, G. *J. Chem. Soc., Dalton Trans.* **1998**, 2779−2781.

(42) (a) Saito, T.; Nakajima, M.; Kobayashi, A.; Sasaki, Y. *J. Chem. Soc., Dalton Trans.* **1978**, 482. Ni···H distances of 1.73(5) and 1.76(6) Å. (b) Segal, B. G.; Lippard, S. J. *Inorg. Chem.* **1977**, *16*, 1623−1629. Ni···H distance of 2.15(3) Å. (c) Carr, N.; Mullica, D. F.; Sappenfield, E. L.; Stone, F. G. A. *Inorg. Chem.* **1994**, *33*, 1666−1673. Ni···H distance of 1.71 Å.

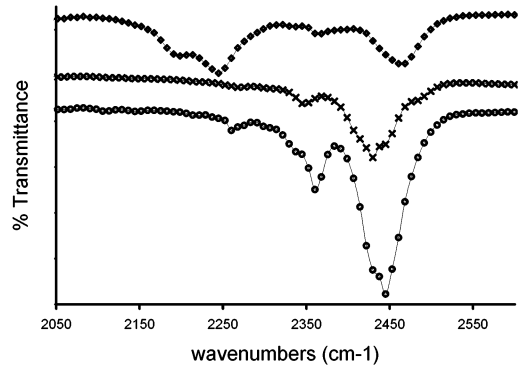

Figure 5. IR spectra of (●) **2**, (×) **3**, and (◆) **4** (KBr disks).

Infrared Spectroscopy. The IR spectra were recorded for the three complexes from 4000 to 400 cm^{-1} to have an insight into the M···H−B interaction. The spectral area containing the B−H stretching (from 2600 to 2050 cm^{-1}) is shown in Figure 5. The IR spectra of **2** and **3** exhibit great similarities, displaying two B−H bands centered at 2446−2362 and 2429s−2347w cm^{-1}, respectively, which are not indicative of a metal−hydride interaction. More interestingly, the IR spectrum of complex **4** in both solution and the solid state shows two distinct sets of bands at 2465−2361 and 2244−2197 cm^{-1}. The two higher-frequency bands can easily be assigned to a terminal B−H stretching, whereas the low-frequency bands support the presence of a Ni···H−B interaction. The splitting of the bands can also be attributed to the *in-phase* and *out-of-phase* stretching of the terminal and coordinated B−H groups, further evidence of their cis arrangement.

Electronic Spectra. To confirm the persistence of the octahedral coordination around the nickel ion in solution, visible and near-infrared electronic spectra of **4** have been recorded in acetonitrile. The complex is characterized by three absorptions [λ/cm^{-1} and ϵ/(M^{-1} cm^{-1})] at $\nu_1 = 8870$ (40) ($^3A_{2g} \rightarrow {}^3T_{2g}$), $\nu_2 = 14\,220$ (78) [$^3A_{2g} \rightarrow {}^3T_{1g}$(F)], and $\nu_3 = 23\,980$ (1120) [$^3A_{2g} \rightarrow {}^3T_{1g}$(P)], as would be expected for a d^8 ion in an octahedral field.[43] The relatively high values of the molar extinction coefficients can be understood by considering the low symmetry of complex **4** (pseudo C_2 symmetry: the twofold axes bisecting the H−Ni−H angle), according to the cis disposition of the two hydrido groups; moreover, owing to the good polarizability of the sulfur donor atoms, a certain degree of covalency in the S−Ni bond could be expected. The Laporte rule could be partially relaxed, increasing the intensities of the d−d transitions.

Ab Initio Calculations. From the structural analysis previously reported, we have noted the presence of two M···H−B interactions for the Ni(II) and Bi(III) complexes and one for the Zn(II) complex. To reveal the nature of these interactions, we have first calculated the equilibrium geometries for all complexes with ONIOM as reported in the Experimental Section. As shown in Tables 3−5, the calculated structures for the Ni(II) and Bi(III) complexes agree very well with the experimental data obtained by X-ray diffraction. A slight increase of the metal−sulfur bond distances is exhibited in both the calculated equilibrium geometries, probably due to the lack of the crystal packing forces present in the solid-state structures. For the Zn(II) complex, the calculated equilibrium geometry did not match with the experimental structure and, therefore, was not considered further.

The second step has been the AIM electron-density-distribution analysis to reveal the presence of a bond between the interacting hydrogen and the metal center. To supply an accurate wave function to the AIM analysis, we have performed a single-point calculation at the same level of theory as that used for the description of the "model system" in the ONIOM partitioning scheme. The AIM analysis is

(43) Lever, A. B. P. *Inorganic Electronic Spectroscopy*, 2nd ed.; Elsevier: Amsterdam, The Netherlands, 1984; pp 507−611.

Table 4. Selected Experimental and Calculated Bond Lengths (Å) and Angles (deg) with the esd in Parentheses for **4a**

molecule I		molecule II		
	X-ray		X-ray	calcd
Ni(1)−S(1)	2.343(1)	Ni(2)−S(5)	2.386(1)	2.242
Ni(1)−S(2)	2.383(1)	Ni(2)−S(6)	2.355(1)	2.502
Ni(1)−S(3)	2.351(1)	Ni(2)−S(7)	2.373(1)	2.424
Ni(1)−S(4)	2.381(1)	Ni(2)−S(8)	2.359(1)	2.493
Ni(1)−H(1)	1.83(4)	Ni(2)−H(5)	1.81(3)	1.847
Ni(1)−H(3)	1.89(3)	Ni(2)−H(7)	1.82(3)	1.850
B(1)−H(1)	1.22(4)	B(3)−H(5)	1.25(3)	1.229
B(1)−H(2)	0.97(4)	B(3)−H(6)	1.06(4)	1.203
B(2)−H(3)	1.18(3)	B(4)−H(7)	1.18(3)	1.229
B(2)−H(4)	1.23(4)	B(4)−H(8)	1.06(3)	1.203
C(11)−S(1)	1.690(4)	C(15)−S(5)	1.684(5)	1.720
C(12)−S(2)	1.704(4)	C(16)−S(6)	1.700(5)	1.715
C(13)−S(3)	1.687(4)	C(17)−S(7)	1.661(5)	1.720
C(14)−S(4)	1.692(4)	C(18)−S(8)	1.684(5)	1.715

molecule I		molecule II	
	X-ray		X-ray
S(1)−Ni(1)−S(2)	97.46(5)	S(5)−Ni(2)−S(6)	99.09(6)
S(1)−Ni(1)−S(3)	89.78(4)	S(5)−Ni(2)−S(7)	171.03(5)
S(1)−Ni(1)−S(4)	90.93(4)	S(5)−Ni(2)−S(8)	87.42(5)
S(1)−Ni(1)−H(1)	90(1)	S(5)−Ni(2)−H(5)	91(1)
S(1)−Ni(1)−H(3)	177(1)	S(5)−Ni(2)−H(7)	86(1)
S(2)−Ni(1)−S(3)	91.84(5)	S(6)−Ni(2)−S(7)	88.22(6)
S(2)−Ni(1)−S(4)	166.15(4)	S(6)−Ni(2)−S(8)	92.10(5)
S(2)−Ni(1)−H(1)	88(1)	S(6)−Ni(2)−H(5)	90(1)
S(2)−Ni(1)−H(3)	83(1)	S(6)−Ni(2)−H(7)	174(1)
S(3)−Ni(1)−S(4)	99.23(5)	S(7)−Ni(2)−S(8)	97.56(6)
S(3)−Ni(1)−H(1)	179(1)	S(7)−Ni(2)−H(5)	84(1)
S(3)−Ni(1)−H(3)	87(1)	S(7)−Ni(2)−H(7)	86(1)
S(4)−Ni(1)−H(1)	82(1)	S(8)−Ni(2)−H(5)	177(1)
S(4)−Ni(1)−H(3)	89(1)	S(8)−Ni(2)−H(7)	91(1)
H(1)−Ni(1)−H(3)	93(2)	H(5)−Ni(2)−H(7)	87(1)
H(1)−B(1)−H(2)	114(3)	H(5)−B(3)−H(6)	114(3)
H(3)−B(2)−H(4)	109(2)	H(7)−B(4)−H(8)	110(2)

Table 5. Experimental and Calculated Distances (Å) and Angles (deg) Involving the M···H−B Interactions for **2a**, **3**, and **4a**

	M···H		M···H−B	
	X-ray	calcd	X-ray	calcd
2a	2.57(3)		129(2)	
	2.86(3)			
3	3.03(4)	2.931	135(3)	132
	2.92(4)	2.780	129(2)	137
4a, molecule I	1.83(4)		141(3)	
	1.89(3)		139(2)	
		1.847		138
		1.850		138
4a, molecule II	1.81(3)		138(3)	
	1.82(3)		146(2)	

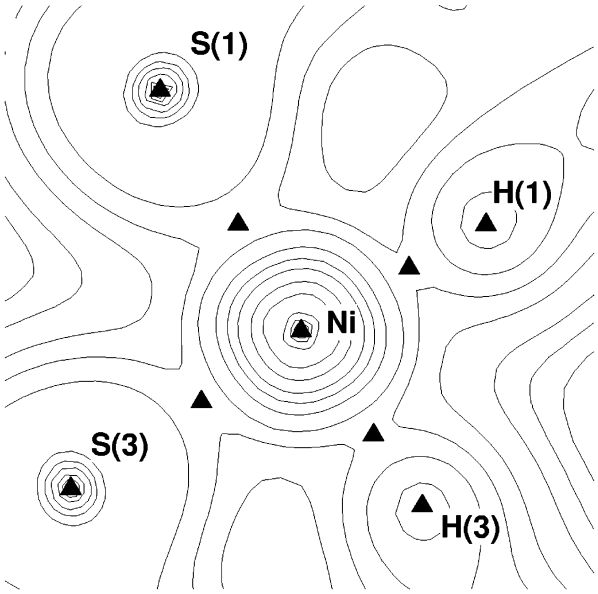

Figure 6. Electron density in the H(1)−Ni−H(3) plane of complex **4**; the triangles between the atoms represent the bond critical points (3, −1).

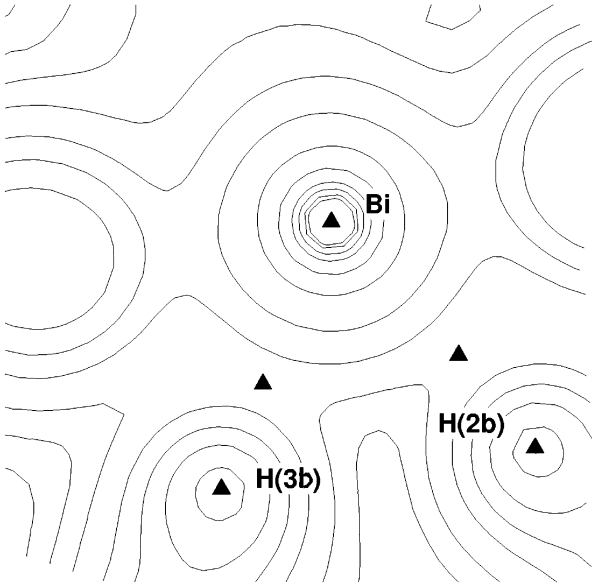

Figure 7. Electron density in the H(2b)−Bi−H(3b) plane of complex **3**; the triangles between the atoms represents the bond critical points (3, −1).

based on a topological characterization of the electron-density distribution and considers the presence of a (3, −1) bond critical point between two atoms as a necessary and sufficient condition for the presence of a chemical bond.[44] The topological analysis of the electron-density distribution in both complexes reveals the presence of such critical points on the Ni−H(1) and Ni−H(2) lines, Bi−H(3b) and Bi−H(2b) lines, and Zn−H(4) line (Figures 6−8). On the other hand, no bond critical point (3, −1) has been found on the Bi−H(1b) and Zn−H(2) lines, indicating the absence of a bond between these atoms. On the basis of these results, we can confirm the existence of a M···H−B interaction, responsible for the trigonal-bipyramidal coordination in **2**,

(44) Bader, R. F. W. *J. Phys. Chem. A* **1998**, *102*, 7314−7323.

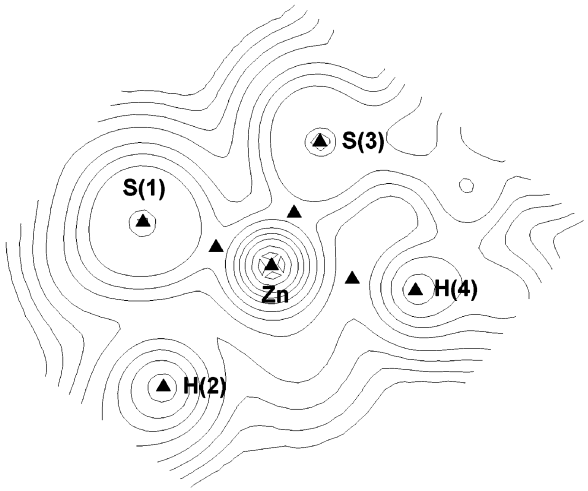

Figure 8. Electron density in the H(4)−Zn−H(2) plane of complex **2**; the triangles between the atoms represents the bond critical points (3, −1).

Table 6. Electron Density, Its Laplacian, and Ellipticity in the Bond Critical Points (3, −1) for Selected Bonds of **3**

bond	ρ (e/au^3)	$\nabla^2\rho$ (e/au^5)	ϵ
Bi−H(3b)	0.012 48	0.007 69	0.055 52
B(3)−H(3b)	0.161 55	−0.030 55	
B(3)−H(3a)	0.169 31	−0.052 27	
Bi−H(2b)	0.009 68	0.006 4	0.18463
B(2)−H(2b)	0.164 67	−0.034 5	
B(2)−H(2a)	0.168 79	−0.051 8	
B(1)−H(1a)	0.171 47	−0.046 7	
B(1)−H(1b)	0.169 24	−0.052 9	
Bi−S(1)	0.030 19	0.008 74	
Bi−S(2)	0.031 72	0.008 73	
Bi−S(3)	0.032 55	0.008 98	
Bi−S(4)	0.031 95	0.009 41	
Bi−S(5)	0.030 86	0.009 19	
Bi−S(6)	0.029 34	0.009 16	

Table 7. Electron Density, Its Laplacian, and Ellipticity in the Bond Critical Points (3, −1) for Selected Bonds of **4**

bond	ρ (e/au^3)	$\nabla^2\rho$ (e/au^5)	ϵ
Ni−H(1)	0.043 07	0.042 74	0.079 81
B(1)−H(1)	0.155 40	−0.047 90	
B(1)−H(2)	0.171 75	−0.058 15	
Ni−H(3)	0.041 87	0.044 18	0.060 76
B(2)−H(3)	0.150 30	−0.029 96	
B(2)−H(4)	0.171 21	−0.055 53	
Ni−S(1)	0.046 42	0.057 25	
Ni−S(2)	0.042 53	0.043 52	
Ni−S(3)	0.050 04	0.052 99	
Ni−S(4)	0.043 31	0.043 83	

and two M···H−B interactions in **3** and **4**, contributing to the dodecahedral and octahedral coordinations, respectively.

It was demonstrated that the value of the electron density ρ and its Laplacian $\nabla^2\rho$ in the bond critical points (3, −1) correlate with the bond energy;[17] a comparison of the M···H−B and M−S bond strengths may also be carried out on the basis of these values. We have, therefore, determined the bond critical points (3, −1) for all the BH−metal and metal−sulfur bonds. The values of the electron densities and its Laplacian in all the obtained bond critical points (3, −1) are reported in Tables 6−8.

The comparison of the ρ and $\nabla^2\rho$ values of the M···H−B interactions for the three complexes denote that the Ni···H interaction is stronger than the Bi···H and Zn···H ones, as

Table 8. Electron Density, Its Laplacian, and Ellipticity in the Bond Critical Points (3, −1) for Selected Bonds of **2**

bond	ρ (e/au^3)	$\nabla^2\rho$ (e/au^5)	ϵ
Zn−H(4)	0.011 57	0.008 55	0.569 04
B(1)−H(1)	0.187 04	−0.043 47	
B(1)−H(2)	0.183 75	−0.022 35	
B(2)−H(3)	0.195 48	−0.031 17	
B(2)−H(4)	0.191 89	−0.010 78	
Zn−S(1)	0.051 45	0.030 15	
Zn−S(2)	0.062 46	0.041 69	
Zn−S(3)	0.055 74	0.035 70	
Zn−S(4)	0.058 75	0.038 14	

Table 9. Natural Atomic Charge Comparison between $Bi(Bt^{Me,Me})_3$ and **3**

atom	$Bi(Bt^{Me,Me})_3$	**3**	atom	$Bi(Bt^{Me,Me})_3$	**3**
H(1a)	−0.040 26	−0.039 55	S(3)	−0.189 09	−0.194 21
H(1b)	−0.053 47	−0.060 10	S(4)	−0.207 67	−0.209 37
H(2a)	−0.040 52	−0.041 06	S(5)	−0.202 89	−0.215 47
H(2b)	−0.078 38	−0.080 39	S(6)	−0.209 30	−0.218 65
H(3b)	−0.084 46	−0.085 75	B(1)	0.298 43	0.301 61
H(3a)	−0.039 20	−0.039 36	B(2)	0.320 54	0.320 96
S(1)	−0.193 92	−0.196 32	B(3)	0.333 83	0.334 04
S(2)	−0.206 05	−0.212 95	Bi	0.986 28	0.985 66

Table 10. Natural Atomic Charges for Complex **4**

atom	charge	atom	charge	atom	charge
H(1)	−0.156 99	B(1)	0.401 13	S(3)	−0.243 35
H(2)	−0.027 62	B(2)	0.402 82	S(4)	−0.244 66
H(3)	−0.158 11	S(1)	−0.242 56	Ni	1.032 07
H(4)	−0.028 92	S(2)	−0.256 11		

Table 11. Natural Atomic Charges for Complex **2**

atom	charge	atom	charge	atom	charge
H(1)	−0.029 31	B(1)	0.272 70	S(3)	−0.428 29
H(2)	−0.068 24	B(2)	0.262 84	S(4)	−0.431 54
H(3)	−0.031 90	S(1)	−0.410 92	Zn	1.427 04
H(4)	−0.075 91	S(2)	−0.385 16		

expected by the observation of the experimental bond distances. Moreover, the positive Laplacian and the small density values would suggest an ionic bond type as defined by Bader.[17]

Observation of the differences between the $\nabla^2\rho$ value of each B−H bond makes it possible to observe the different strengths between the interacting and noninteracting B−H bonds. The latter bond is stronger in all complexes, as shown by the more negative values of $\nabla^2\rho$; this difference is much more evident in the nickel complex, Tables 6−8. The two sets of B−H stretching signals at 2465−2361 and 2244−2197 cm^{-1} in the infrared spectrum of **4** agree very well with the calculated B−H bond-strength difference.

As a direct consequence of the presence of the M···H−B interaction, the atomic charges obtained with the NBO population analysis reported in Tables 9−11 show that the hydrogen atoms participating in this interaction appear more negative than the noninteracting ones. In fact, in the bismuth complex, the noninteracting H(1a) and H(1b) present a smaller difference in their atomic charges. In the Ni(II) complex, the difference between the atomic charges of the interacting and noninteracting hydrogen atoms is much more marked than that in the Bi(III) and Zn(II) complexes, which agrees well with the greater strength of the Ni···H−B interactions. In regards to the zinc complex, the hydrogen atoms pointing toward the metal [H(4) and H(2)] exhibit a greater negative charge than the hydrogen atoms pointing outward [H(1) and H(3)], and a greater negative charge is possessed by the H(4) interacting hydrogen with respect to H(2).

As previously reported, the S−Ni bond lengths are not equivalent because of the bigger trans effect operated by the thioxo sulfur atom with respect to the borohydrido group. The greater values of ρ and the Laplacian in the bond critical points (3, −1) obtained in the Ni−S(1) and Ni−S(3) lines with respect to the values obtained in the Ni−S(2) and Ni−S(4) lines confirm this assumption (Table 7).

For the three complexes, the values of ρ in the bond critical point [M···H] are in the range defined for a classical hydrogen-bond interaction, as proposed by Koch and Popelier; for the Ni(II) complex, $\nabla^2\rho$ is also in accordance with this kind of interaction, whereas, for the Zn(II) and Bi(III) complexes, the values of $\nabla^2\rho$ are smaller than the $\nabla^2\rho$ values reported for a hydrogen bond (interval 0.024−0.139 au).[45] Another important parameter in the description of the hydrogen-bond interaction is the net charge variation as the hydrogen atom becomes more positive once involved in classical hydrogen bonding. In the cases reported here, we assumed that the noninteracting-hydrogen net charge could be approximated to the charges of H(1a) and H(1b) of the bismuth complex because it has been shown that they are not interacting with the metal. As a result, all of the interacting hydrogen atoms become more negative, the net charge increases with the strength of the M···H−B interaction, and it can be inferred that there is a flow of charge from the B−H moiety toward the metals. In regards to the ellipticity of the bond critical point [M···H] (Tables 6−8), for the Ni(II) and Bi(III) complexex, its values agree with a hydrogen-bond typology, whereas, for the zinc complex, the ϵ value is an order of magnitude greater than that for the other M···H−B interactions but smaller than the values reported for an agonistic interaction.[45,46]

On the basis of the previous considerations for ρ, $\nabla^2\rho$, the net charge variation, and the bond ellipticity, the present M···H−B interactions ought to be defined as "inverse hydrogen bonds" in accordance with the results reported by Rozas et al.[47] for similar systems. Also, for the agonistic interaction,[46] the hydrogen atoms involved in the agonistic bond exhibit an increase of the negative charge, but the reported values of ρ and $\nabla^2\rho$ allow us to exclude this kind of interaction for the three complexes.

Conclusions

We have prepared the dihydrobis(thioxotriazolinyl)borato ligand together with its zinc(II), bismuth(III), and nickel(II) complexes, which have been characterized by means of X-ray crystallography and spectroscopy. In all cases, the ligand is

(45) Koch, U.; Popelier, P. L. A. *J. Phys. Chem.* **1995**, *99*, 9747−9754.
(46) (a) Popelier, P. L. A.; Logothetis, G. *J. Organomet. Chem.* **1998**, *555*, 101−111. (b) Sherer, W.; Hieringer, W.; Spiegler, M.; Sirsch, P.; McGrady, G. S.; Downs, A. J.; Haaland, A.; Pedersen, B. *Chem. Commun.* **1998**, 2471−2472.
(47) Rozas, I.; Alkorta, I.; Elguero, J. *J. Phys. Chem. A* **1997**, *101*, 4237−4244.

bound in the S_2 mode, and, for all complexes, the analysis of the structural geometric parameters reveals the presence of M···H−B interactions that are particularly evident for the nickel complex. To better comprehend the role of this interaction for the rationalization of the molecular geometries, ab initio calculations have been performed. Concerning the zinc and bismuth compounds, the tetrahedral/trigonal-bipyramidal and octahedral/dodecahedral geometric ambiguity has been resolved in favor of the trigonal-bipyramidal (zinc) and dodecahedral (bismuth) geometries by using a topological analysis of the electron-density distribution with the AIM method. Despite the long Zn−H and Bi−H intramolecular distances, the AIM analysis has shown the presence of a bond critical point (3, −1), confirming a Zn···H−B and two Bi···H−B interactions. Moreover, on the basis of the topological analysis of the electron density for the three complexes, we consider these interactions as "inverse hydrogen bonds" and not agonistic interactions.

Acknowledgment. This research was supported by the Ministero dell'Università e della Ricerca Scientifica e Tecnologica (Rome, Italy).

Supporting Information Available: Crystallographic information, including full tables of bond lengths and angles, atomic positional parameters, and anisotropic displacement parameters. This material is available free of charge via the Internet at http://pubs.acs.org.

IC025870R